Dihydromyricetin Attenuates Palmitate Acid-Induced Oxidative Stress by promoting Autophagy via SIRT3-ATG4B Signaling in Hepatocytes

Mantian Mi (mi_mantian@sina.com)
Institute of Military Preventive Medcine, Third Military Medical University https://orcid.org/0000-0002-7213-2155

Li Huang
Institude of Military Preventive Medcine, Third Military Medical University

Xianglong Zeng
Institute of Military Preventive Medicine, Third Military Medical University

Bo Li
925 Hospital, Joint Logistics Support Force, PLA

Cong Wang
Institute of Military Preventive Medicine, Third Military Medical University

Min Zhou
Institute of Military Preventive Medcine, Third Military Medical University

Hedong Lang
Institute of Military Preventive Medcine, Third Military Medical University

Long Yi (longgyin8341@hotmail.com)
Institute of Military Preventive Medcine, Third Military Medical University

---

Research

Keywords: dihydromyricetin, NASH, oxidative stress, autophagy, ATG4B, mitochondria, SIRT3

Posted Date: March 17th, 2021

DOI: https://doi.org/10.21203/rs.3.rs-295541/v1

Abstract

Background

Oxidative stress in hepatocytes was an important pathogenesis of nonalcoholic steatohepatitis (NASH). Autophagy was a cellular process that can remove damaged organelles under oxidative stress, and thus presented a potential therapeutic target against NASH. The aim of this work was to investigate whether autophagy participated the protective effects of dihydromyricetin (DHM) on palmitic acid (PA)-induced oxidative stress in hepatocytes and the underlying mechanism.

Methods

HepG2 cells were pretreated with DHM (20 μM) for 2 h, followed by PA (0.2 mM) treatment for 16 h. The oxidative stress was assessed by the quantification of intracellular reactive oxygen species (ROS), mitochondrial ROS (mtROS), mitochondrial membrane potential (MMP) and mitochondrial ultrastructural analyses. The protein expressions of SIRT3, LC3I/II, P62 and ATG4B, as well as the acetylation of AGT4B were determined by western blotting using HepG2 and HepG2/ ATG4B$^{+/-}$ cells with heterozygous knockout of *ATG4B*.

Results

Exposure to PA resulted in increased intracellular ROS and mtROS, decreased MMP and aggravated mitochondrial injury in HepG2 cells, which were notably attenuated by DHM treatment. DHM-induced inhibition of oxidative stress was associated with the induction of autophagy, characterized by upregulated ATG4B and LC3 II as well as downregulated P62 levels. Furthermore, the inhibitory effects of DHM on PA-induced autophagy arrest and oxidative stress were eliminated when pretreated with a SIRT3 inhibitor 3-TYP or conducted in HepG2/ATG4B$^{+/-}$ cells, suggesting that SIRT3 and ATG4B were involved in DHM-induced benefits. Moreover, DHM treatment increased the protein expression of SIRT3 and SIRT3-dependent deacetylation of ATG4B in HepG2 cells.

Conclusion

Our results demonstrated that DHM attenuated PA-induced oxidative stress in hepatocytes through induction of autophagy, which was mediated through the increased expression of SIRT3 and SIRT3-mediated ATG4B deacetylation following DHM treatment.

1. Introduction

Nonalcoholic fatty liver disease (NAFLD) is a spectrum of liver disease that is becoming the main cause of chronic liver disease, with a prevalence as high as one quarter of the population [1]. Nonalcoholic steatohepatitis (NASH) is believed to be a more advanced liver pathologies, which could progress to hepatic fibrosis, cirrhosis and even hepatocellular carcinoma (HCC). According to the “two-hit theory”, liver steatosis (the “first hit”) induces fat accumulation, followed by oxidative stress (the “second hit”) which leads to proinflammatory molecules release, mitochondrial damage and lipid peroxidation [2]. The consequential surplus of lipids in hepatocytes leads to lipotoxicity and oxidative stress, which promotes mitochondrial dysfunction through multiple mechanisms including augmented reactive oxygen species (ROS) production and decreased mitochondrial membrane potential (MMP) [3]. Much evidence suggests that oxidative stress, which promotes mitochondrial dysfunction especially in hepatocytes, represents a key element in driving hepatic inflammation in NASH, leading to hepatocyte dysfunction or death [4]. Thus, protecting hepatocytes against oxidative stress and maintaining redox homeostasis is important to reverse or retard the progression of NASH.

Autophagy, a conserved cellular process, can reduce oxidative stress by degrading cytoplasm and damaged organelles, such as mitochondria, through lysosomes or vacuoles to maintain cellular environment homeostasis [5]. Much evidence indicates that NASH is accompanied by decreased autophagy and increased oxidative stress [6–8]. Autophagy-related 4B cysteine peptidase (ATG4B) is the most active protease among the four mammalian paralogs of ATG4, which acts an important role in the regulation of autophagy [9, 10]. Evidence indicates that ATG4B can be acetylated at the site of N-terminus, which is one of the major protein modifications in eukaryotes [11]. Up to date, the underlying mechanisms of ATG4B and its acetylation in the development and progression of NASH remains unknown.

SIRT3, a member of the mammalian sirtuin family protein that is localized to mitochondria, has robust deacetylase activity and plays an important role in the regulation of metabolic homeostasis and energy metabolism [12]. With dysregulated protein acetylation in the mitochondria, *SIRT3* knockout mice fed with high-fat diet exhibited aggravated metabolic syndrome [13]. And overexpression of *SIRT3* preserved electron transport chain, enhanced adenosine triphosphate generation and strengthened autophagy [12, 14–16]. However, a recent study demonstrated that overexpression of SIRT3 inhibited adenosine monophosphate-activated protein kinase and rapamycin C1 activation, leading to autophagy suppression [17]. These differing results raise the question that whether SIRT3 could be a critical regulator of autophagy in NASH.

Dihydromyricetin (DHM) is a natural flavonoid compound which mainly exists in *Ampelopsis grossedentata* [18]. In our previous study, DHM supplementation promoted lipid metabolism in NAFLD patients [19], attenuated hepatic steatosis and maintained redox homeostasis through increased SIRT3 expression [20]. Previous researches have showed that DHM could induce autophagy in HepG2 cells [21–23]. Thus, we hypothesized that DHM might attenuate oxidative stress by regulating autophagy in hepatocytes. As expected, these data provided new evidence that DHM significantly inhibited oxidative stress in hepatocytes through induction of autophagy via SIRT3-ATG4B signaling pathway.

2. Materials And Methods

2.1. Reagents

DHM (CAS No. 27200-12-0, HPLC ≥ 98%) was obtained from Chengdu Mansite Bio-Technology (Chengdu, China). Fetal bovine serum (FBS) and Dulbecco's modified Eagle's medium (DMEM) were purchased from Gibco (Carlsbad, CA, USA). Dimethyl sulfoxide (DMSO) and palmitate acid (PA) were obtained from Sigma-Aldrich (St. Louis, MO, USA). Penicillin/streptomycin and bovine serum albumin (BSA) were obtained from Beyotime (Shanghai, China). Antibodies against acetyl-lysine (AcK), voltage-dependent anion channel (VDAC), P62 and LC3 were purchased from Cell Signaling Technology (Beverly, MA, USA). Antibodies against beta-actin (ACTB), ATG4B, and SIRT3 were obtained from Abcam (Cambridge, MA, USA). Antibody against optic atrophy 1 protein (OPA1) was purchased from BD Biosciences (San Jose, CA, USA). Chloroquine (CQ), 3-methyladenine (3-MA) and 3-(1H-1, 2, 3-triazol-4-yl) pyridine (3-TYP, CAS No. 120241-79-4) were purchased from MedChemExpress (Monmouth Junction, NJ, USA). Other reagents were purchased as indicated in the corresponding methods.

2.2. Cell culture and treatments

HepG2 cell line was provided from the American Type Culture Collection (Manassas, VA, USA). HepG2/ATG4B$^{+/-}$ cell line, in which *ATG4B* was heterozygous knockout with CRISPR-Cas9 system, was a gift from Nan Zhang (Department of Biochemistry and Molecular Biology, College of Basic Medical Sciences, Third Military Medical University, Chongqing 400038, China) [24]. Both HepG2 and HepG2/ATG4B$^{+/-}$ cell lines were cultured in DMEM medium with 10% FBS, 1% penicillin/streptomycin at 37°C and 5% CO_2 incubator, and cells from the 3rd to 6th passages were used for the experiments. To detect the effect of DHM on PA-induced oxidative stress in hepatocytes, both cell lines were pretreated with DHM (20 μM) or the vehicle (0.5% DMSO) for 2 h prior to the treatment of PA (0.2 mM) for an additional 16 h as described previously [20]. To determine the involvement of autophagy and SIRT3 in DHM-induced inhibition of oxidative stress in hepatocytes, the autophagy inhibitor 3-MA (0.5 mM) and CQ (20 μM) as well as a SIRT3 inhibitor 3-TYP (50 μM) were used 1 h prior to DHM treatment, respectively.

2.3. Green fluorescent protein (GFP)-LC3 transfection

After seeded on cell culture dish (NEST, China) for 8 h, HepG2 cells were transfected with GFP-LC3 expression vector (kindly provided by MengYu Liu, Department of Occupational Health, Third Military Medical University, Chongqing 400038, China) at the final concentration of 1 μg/μL for 4 h using Lipofectamine 2000 (Invitrogen, Carlsbad, CA) according to the manufacturer's instructions. Samples were then analyzed using the laser confocal scanning microscopy (Zeiss, Germany).

2.4. Immunofluorescence microscopy analysis

HepG2 cells were loaded with MitoTracker Red (500 nM, Cell Signaling Technology, USA) to label the mitochondria as described[25]. Briefly, after treated as indicated, the HepG2 cells were loaded with

MitoTracker Red and imaged by laser confocal scanning microscopy (Zeiss, Germany) under the excitation (Ex) and emission (Em) wavelength of 644 nm and 665 nm, respectively. To observe the mitochondrial fusion, HepG2 cells were labeled with MitoTracker Red and then fixed with 4% paraformaldehyde (Beyotime, China), permeabilized with 0.25% Triton X-100 (Beyotime, China) and blocked with 5% goat serum (Beyotime, China). Then, cells were incubated with primary antibody against OPA1 at 4°C overnight, and incubated with Alexa Fluor® 488 goat anti-rabbit IgG secondary antibody (1:200, Beyotime, China). Finally, nuclei were counterstained with DAPI. Samples were analyzed using the laser confocal scanning microscopy (Zeiss, Germany).

2.5. Intracellular and mitochondrial ROS assessment

The intracellular and mitochondrial ROS (mtROS) levels were determined using DCFH-DA (Beyotime, China) and MitoSOX™ Red (Invitrogen, Carlsbad, CA) according to the manufacturer's instructions, respectively. After treated as indicated, cells were loaded with DCFH-DA (10 μM) in FBS-free DMEM at 37°C for 30 min, then washed twice with FBS-free DMEM to detect the intracellular ROS level. Meanwhile, cells were loaded with MitoSOX™ Red (5 μM) at 37°C for 30 min, then washed gently three times with warm PBS to detect the mtROS level. The mean fluorescence intensity of intracellular ROS (Ex/Em: 488/525 nm) and mtROS (Ex/Em: 510/580 nm) were determined using flow cytometry (FCM; Accuri C6, BD Biosciences, San Jose, CA), respectively.

2.6. MMP measurement

The MMP was measured using JC-1 probe (Beyotime, China, CAS No. 47729-63-5) according to the manufacturer's instruction. Briefly, after treated as indicated, cells were loaded with JC-1, followed by washing twice in PBS before being subjected to FCM for green fluorescence (Ex/Em: 488/525 nm) and red fluorescence (Ex/Em: 525/590 nm) (Accuri C6, BD Biosciences, San Jose, CA). Fluorescence intensity ratio was calculated to reflect the MMP.

2.7. Transmission electron microscopy (TEM)

The mitochondrial morphology was observed by a TEM. Briefly, HepG2 cells were treated as described previously [25] and visualized on TEM (EM420, Amsterdam, The Netherlands). Three samples per group and ten images of each sample were selected for quantitative analysis. Any types of ultrastructural changes including broken inner and outer membranes, intramitochondrial edema, disrupted cristae, hypertrophic giant mitochondria as well as intramitochondrial edema were considered damaged and dysfunctional mitochondria. The ratio of the number of normal mitochondria to the total was calculated to evaluate the percentage of normal mitochondria.

2.8. Western blotting and co-immunoprecipitation (Co-IP)

Cells were lysed in cell lysis buffer (Sigma-Aldrich, St. Louis, MO, USA) containing 1% protease inhibitor cocktail and phosphatase inhibitor cocktail (Roche, Basel, Switzerland). The mitochondrial proteins were extracted using a Cell Mitochondria Isolation Kit (Beyotime, China) with protein concentrations determined using a BCA kit (Beyotime, China), and samples mixed with loading buffer (Beyotime, China)

were heated at 100°C for 10 min. For Western blotting, equal amounts of proteins were resolved via SDS-PAGE (10%-15%), followed by transfer and fixation on polyvinylidene difluoride membranes (0.22 μm; Millipore, Billerica, MA, USA). The membranes were blocked with 5% skimmed milk for 2 h and then immunoblotted with antibodies (1:1000) overnight at 4°C. Then, the membranes were washed with tris-buffered saline with Tween (TBST) buffer three times, followed by the incubation with the appropriate secondary antibody (Sigma-Aldrich, St. Louis, MO, USA) (1:5000) for 1 h and then washing with TBST buffer three times. The immunostained bands were visualized and determined using Fusion FX (Vilber Lourmat, France) and Immobilon Western Chemiluminescent HRP Substrate (Millipore, USA). ACTB and VDAC were used as loading controls for whole cell lysates and mitochondrial lysates, respectively. Densitometry analysis was carried out using ImageJ software. For Co-IP analysis, the proteins were diluted in lysis buffer and then mixed with the corresponding antibodies as well as protein A/G-agarose bead slurry (Cell Signaling Technology, Beverly, MA, USA) overnight at 4°C with gentle rotation. Then, the mixtures were centrifuged at 1100×g for 3 min at 4°C and washed with lysis buffer five times followed by Western blotting for immunoblotting. The specificity of antibodies used for immunoprecipitation was routinely validated by running negative controls with non-immune IgG under the same conditions.

2.9. Statistical analysis

Data analysis was performed with SPSS 19.0 software (Chicago, IL, USA). All experimental data were expressed as mean ± SD of at least 3 experiments. Statistical differences among groups were determined with either Student's t-test (for two groups) or one-way analysis of variance (ANOVA) followed by LSD post hoc tests (for multiple group comparisons). A p value less than 0.05 was considered to indicate statistically significant difference; ns means not significant.

3. Results

3.1. DHM inhibits PA-induced oxidative stress in hepatocytes

To clarify the effects of DHM on PA-induced oxidative stress in hepatocytes, HepG2 cells were labeled with DCFH-DA probe and qualified it by FCM to determine the intracellular ROS level. As shown in Fig. 1A-B, the intracellular ROS level in the PA-treated group was significantly increased compared with the control group. However, DHM notably suppressed PA-induced increase of intracellular ROS. HepG2 cells were then labeled with MitoSOX™ Red to determine the mtROS levels. As shown in Fig. 1C-D, DHM treatment dominantly inhibited PA-induced mitochondria-derived ROS level in HepG2 cells. The MMP is a key parameter for evaluation of mitochondrial function, which was usually detected using JC-1 fluorescent probe. As shown in Fig. 1E-F, DHM treatment significantly inhibited PA-induced decrease of MMP in hepatocytes.

The normal structure and function of mitochondria are closely related to the redox homeostasis [26]. Filamentous and tubular mitochondria are widely agreed to be healthy, while mitochondria that are

fragmented and spherical in appearance are considered to be structurally and functionally abnormal [26]. In the study, HepG2 were labeled with MitoTracker Red to evaluate the changes of mitochondrial structure (Fig. 1G). In PA-induced HepG2 cells, the mitochondria seemed mostly fragmented or spherical in appearance, suggesting a certain degree of dysfunction. However, when cells were pretreated with DHM, the mitochondria were considerably improved, with a notably tubular shape. The results indicated that DHM treatment resulted in an improvement in mitochondrial structure and function in PA-treated hepatocytes. To further characterize the mitochondrial ultrastructure, cells were detected by TEM. As shown in Fig. 1H, the mitochondria appeared to be swollen and round-shaped with disrupted mitochondrial cristae (red arrow) in PA-treated HepG2 cells. Whereas, DHM-treated HepG2 cells showed improved mitochondrial ultrastructure with relatively less swollen and more organized mitochondrial cristae (Fig. 1H). Interestingly, the formation of autophagosome (blue arrow) was observed in the DHM-pretreated HepG2 cells, suggesting a dominant induction of autophagy by DHM treatment. Moreover, DHM treatment resulted in an obviously increased percentage of normal mitochondria compared to PA-induced hepatocytes, implying its role in the prevention against PA-induced injury in hepatocytes (Fig. 1I). Moreover, the expression of OPA1, which is responsible for the regulation of mitochondrial fusion, was measured. It was found that PA induced a lowered OPA1 expression in hepatocytes, which was significantly inhibited by DHM treatment **(Fig. S1)**. Overall, these results indicate that DHM could inhibit PA-induced oxidative stress and maintain normal mitochondrial structure in PA-induced hepatocytes.

3.2. DHM suppresses PA-induced oxidative stress by induction of autophagy in hepatocytes

Previous studies reported that the occurrence of NAFLD involves with mitochondrial dysfunction of hepatocytes, which is associated with autophagy arrest [27]. To determine whether DHM has an impact on autophagy in PA-induced hepatocytes, HepG2 cells were exposed to different concentrations (5, 10, 20, 40, 80 μM) of DHM alone for 16 h. As shown in Fig. 2A-B, the protein expression of ATG4B was significantly upregulated as the increased concentrations of DHM. Moreover, treatment with DHM at a higher concentration (≥ 20 μM) resulted in a decreased expression of P62 and an increased expression of LC3 II (Fig. 2A, C-D), suggesting that DHM alone could promote autophagic flux in hepatocytes. To further investigate the influence of DHM on autophagy in PA-induced hepatocytes, autophagy inhibitors of CQ (20 μM) and 3-MA (5 mM) were applied as indicated (Fig. 2E-G). As shown in Fig. 2E-G, PA treatment induced increased P62 and decreased LC3 II levels, and these effects were significantly suppressed by DHM treatment. However, the inhibitory effects of DHM on PA-induced autophagic flux decrease was substantially suppressed by the addition of 3-MA and CQ separately. Furthermore, DHM significantly inhibited PA-induced intracellular ROS and mtROS levels in HepG2 cells, as shown in Fig. 2H-K. However, pretreatment with 3-MA and CQ dominantly eliminated DHM-induced amelioration on the oxidative stress in HepG2 cells (Fig. 2H-K). DHM-induced amelioration of MMP in PA-treated hepatocytes was also blocked by the addition of 3-MA and CQ separately (Fig. 2L-M). Besides, pretreatment with DHM resulted in a significantly increase of GFP-LC3 puncta in HepG2 cells (Fig. 2N). Taken together, these findings demonstrate that DHM inhibits PA-induced oxidative stress by induction of autophagy in hepatocytes.

3.3. DHM attenuates PA-induced autophagy arrest and oxidative stress in hepatocytes via SIRT3

It was demonstrated that SIRT3 overexpression is involved in the activation of autophagy and mitophagy in myocyte [28, 29]. SIRT3 was also found to be a key molecule responsible for the suppression of intracellular ROS level by deacetylation of mitochondrial enzymes [30]. In order to determine whether SIRT3 is involved with the inhibitory effects of DHM on PA-induced autophagy arrest and oxidative stress in hepatocytes, the SIRT3 inhibitor 3-TYP was used as indicated. As shown in Fig. 3A-C, western blotting analysis indicated that the protein expression of P62 was increased and that of LC3 II was decreased in PA-treated hepatocytes, implying that PA notably suppressed autophagy in HepG2 cells. However, PA-induced autophagy inhibition was significantly attenuated by DHM treatment, and this effect was predominantly eliminated by the addition of 3-TYP (Fig. 3A-C). These results suggested that SIRT3 was involved in the regulation of autophagic flux in DHM-treated HepG2 cells. Moreover, DHM treatment suppressed the increase of intracellular ROS (Fig. 3D-E) and mtROS (Fig. 3F-G) as well as decreased MMP (Fig. 3H-I) in PA-induced hepatocytes. However, these effects were abolished by a SIRT3 inhibitor 3-TYP pretreatment. These findings indicate that DHM treatment attenuates PA-induced autophagy arrest and oxidative stress in hepatocytes, which was mediated via SIRT3.

3.4. DHM attenuates PA-induced autophagy arrest and oxidative stress in hepatocytes partially through ATG4B

ATG4B is a cysteine protease which acts a significant role in the regulation of autophagy process [31]. Pervious findings indicated that DHM treatment alone could upregulate the expression of ATG4B in HepG2 cells (Fig. 2A-B). We therefore suspected that ATG4B might also be involved in DHM-mediated modulation of autophagy and oxidative stress in PA-induced hepatocytes. We conducted experiments using HepG2/ATG4B$^{+/-}$ cells with heterozygous knockout of *ATG4B* in HepG2 cell line **(Fig. S2)**. Our data indicated that DHM treatment resulted in a decreased P62 and increased LC3 II levels in HepG2 cells (Fig. 2A-C). However, these effects were blocked in HepG2/ATG4B$^{+/-}$ cells, suggesting that ATG4B was essential for DHM-induced autophagy in hepatocytes (Fig. 4A-C). Similarly, DHM suppressed the increase of intracellular ROS (Fig. 4D-E) and mtROS (Fig. 4F-G) levels as well as loss of MMP (Fig. 4H-I) in HepG2 cells, which were abolished in HepG2/ATG4B$^{+/-}$ cells, suggesting that ATG4B was essential for DHM-induced inhibition of oxidative stress in hepatocytes. In conclusion, these results indicate that DHM suppressed PA-induced autophagy arrest and oxidative stress in hepatocytes, which might be mediated partially through ATG4B.

3.5. DHM facilitates SIRT3-mediated deacetylation of ATG4B in hepatocytes

Based on the findings that SITR3 and ATG4B might play crucial roles in DHM-mediated amelioration of oxidative stress in hepatocytes, the underling mechanisms need to be further clarified. We assumed that DHM could promote autophagy through SIRT3-mediated deacetylation of ATG4B in HepG2 cells. As

shown in Fig. 5A-B, DHM treatment significantly inhibited PA-induced hyperacetylation in HepG2 cells, accompanied by increased SIRT3 expression, implying a critical role of SIRT3 in DHM-induced deacetylation (Fig. 5A-B). Furthermore, it was reported that the N-terminus of ATG4B could be post-translational modified by acetylation[11]. As SIRT3 has robust deacetylase activity in mitochondria [12], we hypothesized that SIRT3 could modulate the deacetylation of ATG4B. As shown in Fig. 5C, SIRT3 could be co-immunoprecipitated with ATG4B by the Co-IP assay. Next, we sought to investigate whether ATG4B could be modulated by SIRT3-mediated deacetylation in HepG2 cells. As shown in Fig. 5D-E, the immunoprecipitated ATG4B was incubated with a specific antibody against acetyllysine residues, it was showed that PA treatment led to an increased acetylation of ATG4B in hepatocytes, which was enhanced by a SIRT3 inhibitor 3-TYP pretreatment. Moreover, DHM treatment inhibited PA-induced increase of ATG4B acetylation in HepG2 cells, as shown in Fig. 5F-G. In conclusion, DHM facilitates SIRT3-mediated deacetylation of ATG4B in hepatocytes.

Discussion

NAFLD is characterized by a wide spectrum of liver disorders, ranging from simple steatosis in hepatocytes to NASH, liver fibrosis and cirrhosis, and has been the most common cause of chronic liver disease in western countries [1]. According to the classical “two-hit theory”, hepatic fat accumulation (the “first hit”) followed by elevated output of oxidative stress (the “second hit”) leads to exaggerated inflammation in the liver, eventually leading to NASH and fibrosis [2]. At present, there are no approved pharmacological treatments, due to significant issues with efficacy and long-term safety [7]. Thus, dietary strategies for the prevention and the treatment of NAFLD are strongly recommended. Accumulating evidence indicates that several polyphenols contribute to the enhancement of lipid accumulation and oxidative stress of the liver, and are considered to be associated with a low prevalence of metabolic diseases, including insulin resistance, hypertension, and NASH [32-34]. Thus, encouragement of consumption of polyphenol-rich diets is beneficial for the prevention and treatment of NASH. Our previous research has demonstrated that DHM, as a major flavonoid in *Ampelopsis grossedentata*, was effective at improving lipid metabolism in NAFLD patients [19]. And DHM could effectively ameliorate PA-induced steatosis in hepatocytes through improving mitochondrial respiratory chain function and antioxidant capacity via SIRT3 [20]. However, the effects of DHM on oxidative stress in hepatocytes and the underlying mechanisms have not been fully clarified. In this study, we found that DHM significantly attenuated PA-induced oxidative stress in hepatocytes through induction of autophagy, and the benefits were mediated through the deacetylation of ATG4B via increased SIRT3 expression **(Fig. 6)**. Our results provided new insights into a SIRT3-mediated mechanism involving DHM-induced amelioration of oxidative stress in hepatocytes, indicating that SIRT3/ATG4B-mediated induction of autophagy might play an important role in the attenuation of oxidative stress in hepatocytes.

Various studies have indicated that the mechanisms involved in progression of NASH were related to increased ROS and oxidative stress [7]. Pro-oxidant systems, including cyclooxygenase, lipoxygenase, cytochrome P450, and free radical products, have been implicated, individually or cooperatively, as being involved in the production of oxidative stress in NASH. More importantly, mitochondria are critical

important in ROS overproduction, which leads to mitochondrial dysfunction and abnormal respiration, culminating in NAFLD occurrence and development [7]. In the current study, we found that DHM treatment decreased the intracellular and mitochondrial ROS levels in hepatocytes, which was associated with improved mitochondrial structure and function, indicating a key role of DHM in the maintenance of liver redox homeostasis.

Autophagy is a conserved cellular process that affects organisms as diverse as worms, flies, yeast, and mammals [5]. The best-characterized functions of autophagy include provision of an alternative source of energy during starvation and maintenance of cellular quality control [35]. There is accumulating evidence demonstrating that autophagy may protect against steatosis as well as promote hepatocyte regeneration by limiting hepatocyte injury and reducing M1 polarization [36, 37]. Previous research has indicated that DHM can induce autophagy in HepG2 cells [23]. Here, we demonstrated that DHM treatment inhibited the PA-induced autophagic flux decrease in hepatocytes, thereby resulting in the removal of depolarized and damaged mitochondria, finally leading to reduced oxidative stress in hepatocytes. This finding indicates that autophagy plays a significant role in DHM-induced inhibition of oxidative stress in hepatocytes.

SIRT3, which is localized in the mitochondria can regulate energy metabolism and metabolic homeostasis through its deacetylase activity [12]. Some studies have reported that both increased oxidative stress and damaged mitochondria were associated with decreased SIRT3 levels, and that SIRT3 deficiency leads to increased intracellular ROS levels [38-40]. We previously found that SIRT3 could be upregulated by DHM treatment, and SIRT3 enrichment could promote mitochondrial respiratory capacity and maintenance of redox homeostasis in NAFLD [20, 41]. In this study, the protective effects of DHM in PA-induced HepG2 cells were blocked by 3-TYP treatment. Our results indicate that DHM can inhibit PA-induced oxidative stress through SIRT3-mediated autophagy induction.

It is widely accepted that ATG4 cysteine protease acts a significant role in the processing of ATG8 protein during autophagy[42]. We found that the expression of ATG4B was upregulated by DHM treatment. Additionally, the protective effects of DHM on PA-induced oxidative stress as well as autophagic flux reduction were eliminated in HepG2/ATG4B$^{+/-}$ cells, indicating that ATG4B might play a significant role in DHM-mediated oxidative stress homeostasis. Several studies have demonstrated that low levels of ROS could regulate ATG4A and ATG4B at cysteine 81 and 78, respectively[43-45]. However, we found that increased ROS levels were accompanied with a decrease in ATG4B in PA-treated hepatocytes. Further research is needed to explore the association between ROS and ATG4B in hepatocytes. Meanwhile, it is difficult to elucidate the role of SIRT3 which localized in the mitochondria in de-acetylating cytosolic protein, ATG4B. One possible explanation is during the process of mitophagy, ATG4B bound to SIRT3 and de-acetylated after recruited close to mitochondria. Meanwhile, impaired autophagy might result in an accumulation of damaged mitochondria and exacerbating mitochondrial oxidative stress. Accordingly, the use of DHM attenuated oxidative stress and promoted autophagy.

Conclusion

In summary, our results suggest that DHM attenuates PA-induced oxidative stress in HepG2 cells. And the beneficial effects were involved with the increased expression of SIRT3 and the interaction between SIRT3 and ATG4B, thereby leading to the deacetylation of ATG4B and the induction of autophagy. Our results provide new evidence of the links among oxidative stress, autophagy and SIRT3, which are also helpful for a better understanding of DHM-mediated preventive and therapeutic effects against oxidative stress in hepatocytes during NAFLD progression.

Abbreviations

3-MA, 3-methyladenine; 3-TYP, 3-(1H-1, 2, 3-triazol-4-yl) pyridine; AcK, acetyl-lysine; ACTB, beta-actin; ATG4B, autophagy-related 4B cysteine peptidase; Co-IP, co-immunoprecipitation; CQ, chloroquine; DHM, dihydromyricetin; HepG2, human hepatocellular cancer cell line; LC3, light chain 3; MMP, mitochondrial membrane potential; mtROS, mitochondrial reactive oxygen species; NAFLD, nonalcoholic fatty liver disease; NASH, nonalcoholic steatohepatitis; OPA1, optic atrophy 1 protein; PA, palmitate acid; P62/SQSTM1, sequestosome 1; ROS, reactive oxygen species; SIRT3, silent mating type information regulation 2 homolog-3; VDAC, voltage-dependent anion channel.

Declarations

Ethics approval and consent to participate

Not applicable.

Consent for publication

Not applicable.

Availability of data and materials

All data generated or analyzed during this study are included in this published article or are available from the corresponding author on reasonable request.

Competing interests

The authors declare that they have no competing interests

Funding

This work was supported by National Natural Science Foundation of China (grant number: 81903317).

Authors' contributions

MMT, XZ and BL designed the study; LH, XZ, CW, HDL and MZ conducted the experiments; LH and XZ did sample analysis and data analysis; LH wrote the

Manuscript; MMT and LY revised the paper. All authors read and approved the final manuscript.

Acknowledgements

We thank Dr. Mengyu Liu for GFP-LC3 expression vector and Dr. Nan Zhang for HepG2/ATG4B$^{+/-}$ cell line. We also thank the technicians in Biological Testing Center of Third Military Medical University for their assistance in experiments.

References

1. Younossi Z, Anstee QM, Marietti M, Hardy T, Henry L, Eslam M, et al. Global burden of NAFLD and NASH: trends, predictions, risk factors and prevention. Nature reviews Gastroenterology hepatology. 2018;15:11–20.
2. Day CP, James OF. Steatohepatitis: a tale of two "hits"? Gastroenterology. 1998;114:842–5.
3. Li R, Xin T, Li D, Wang C, Zhu H, Zhou H. Therapeutic effect of Sirtuin 3 on ameliorating nonalcoholic fatty liver disease: The role of the ERK-CREB pathway and Bnip3-mediated mitophagy. Redox Biol. 2018;18:229–43.
4. Simões ICM, Fontes A, Pinton P, Zischka H, Wieckowski MR. Mitochondria in non-alcoholic fatty liver disease. Int J Biochem Cell Biol. 2018;95:93–9.
5. Mizushima N. Autophagy: process and function. Genes Dev. 2007;21:2861–73.
6. Khambu B, Yan S, Huda N, Liu G, Yin XM. Autophagy in non-alcoholic fatty liver disease and alcoholic liver disease. Liver research. 2018;2:112–9.
7. Spahis S, Delvin E, Borys JM, Levy E. Oxidative Stress as a Critical Factor in Nonalcoholic Fatty Liver Disease Pathogenesis. Antioxid Redox Signal. 2017;26:519–41.
8. González-Rodríguez A, Mayoral R, Agra N, Valdecantos MP, Pardo V, Miquilena-Colina ME, et al. Impaired autophagic flux is associated with increased endoplasmic reticulum stress during the development of NAFLD. Cell death disease. 2014;5:e1179.
9. Tanida I, Sou YS, Minematsu-Ikeguchi N, Ueno T, Kominami E. Atg8L/Apg8L is the fourth mammalian modifier of mammalian Atg8 conjugation mediated by human Atg4B, Atg7 and Atg3. FEBS J. 2006;273:2553–62.
10. Li M, Hou Y, Wang J, Chen X, Shao ZM, Yin XM. Kinetics comparisons of mammalian Atg4 homologues indicate selective preferences toward diverse Atg8 substrates. J Biol Chem. 2011;286:7327–38.
11. Zhang L, Li J, Ouyang L, Liu B, Cheng Y. Unraveling the roles of Atg4 proteases from autophagy modulation to targeted cancer therapy. Cancer letters. 2016;373:19–26.
12. Ahn BH, Kim HS, Song S, Lee IH, Liu J, Vassilopoulos A, et al. A role for the mitochondrial deacetylase Sirt3 in regulating energy homeostasis. Proc Natl Acad Sci USA. 2008;105:14447–52.
13. Hirschey MD, Shimazu T, Jing E, Grueter CA, Collins AM, Aouizerat B, et al. SIRT3 deficiency and mitochondrial protein hyperacetylation accelerate the development of the metabolic syndrome.

Molecular cell. 2011;44:177–90.

14. Dai SH, Chen T, Li X, Yue KY, Luo P, Yang LK, et al. Sirt3 confers protection against neuronal ischemia by inducing autophagy: Involvement of the AMPK-mTOR pathway. Free Radic Biol Med. 2017;108:345–53.
15. Hallows WC, Lee S, Denu JM. Sirtuins deacetylate and activate mammalian acetyl-CoA synthetases. Proc Natl Acad Sci USA. 2006;103:10230–5.
16. Kim SC, Sprung R, Chen Y, Xu Y, Ball H, Pei J, et al. Substrate and functional diversity of lysine acetylation revealed by a proteomics survey. Molecular cell. 2006;23:607–18.
17. Li S, Dou X, Ning H, Song Q, Wei W, Zhang X, et al. Sirtuin 3 acts as a negative regulator of autophagy dictating hepatocyte susceptibility to lipotoxicity. Hepatology. 2017;66:936–52.
18. Gao JH, Liu BG, Ning ZX, Zhao RX, Zhang AY, Wu Q. CHARACTERIZATION AND ANTIOXIDANT ACTIVITY OF FLAVONOID-RICH EXTRACTS FROM LEAVES OF AMPELOPSIS GROSSEDENTATA. J Food Biochem. 2009;33:808–20.
19. Chen S, Zhao X, Wan J, Ran L, Qin Y, Wang X, et al. Dihydromyricetin improves glucose and lipid metabolism and exerts anti-inflammatory effects in nonalcoholic fatty liver disease: A randomized controlled trial. Pharmacological research. 2015;99:74–81.
20. Zeng X, Yang J, Hu O, Huang J, Ran L, Chen M, et al. Dihydromyricetin Ameliorates Nonalcoholic Fatty Liver Disease by Improving Mitochondrial Respiratory Capacity and Redox Homeostasis Through Modulation of SIRT3 Signaling. Antioxidants & redox signaling. 2018.
21. Qiu P, Dong Y, Li B, Kang XJ, Gu C, Zhu T, et al. Dihydromyricetin modulates p62 and autophagy crosstalk with the Keap-1/Nrf2 pathway to alleviate ethanol-induced hepatic injury. Toxicology letters. 2017;274:31–41.
22. Shi L, Zhang T, Zhou Y, Zeng X, Ran L, Zhang Q, et al. Dihydromyricetin improves skeletal muscle insulin sensitivity by inducing autophagy via the AMPK-PGC-1α-Sirt3 signaling pathway. Endocrine. 2015;50:378–89.
23. Xia J, Guo S, Fang T, Feng D, Zhang X, Zhang Q, et al. Dihydromyricetin induces autophagy in HepG2 cells involved in inhibition of mTOR and regulating its upstream pathways. Food chemical toxicology: an international journal published for the British Industrial Biological Research Association. 2014;66:7–13.
24. Zhang N, Wu Y, Lyu X, Li B, Yan X, Xiong H, et al. HSF1 upregulates ATG4B expression and enhances epirubicin-induced protective autophagy in hepatocellular carcinoma cells. Cancer letters. 2017;409:81–90.
25. Yang J, Zhou X, Zeng X, Hu O, Yi L, Mi M. Resveratrol attenuates oxidative injury in human umbilical vein endothelial cells through regulating mitochondrial fusion via TyrRS-PARP1 pathway. Nutrition metabolism. 2019;16:9.
26. Eisner V, Picard M, Hajnóczky G. Mitochondrial dynamics in adaptive and maladaptive cellular stress responses. Nat Cell Biol. 2018;20:755–65.

27. Zhou H, Du W, Li Y, Shi C, Hu N, Ma S, et al. Effects of melatonin on fatty liver disease: The role of NR4A1/DNA-PKcs/p53 pathway, mitochondrial fission, and mitophagy. Journal of pineal research. 2018;64.
28. Yu W, Gao B, Li N, Wang J, Qiu C, Zhang G, et al. Sirt3 deficiency exacerbates diabetic cardiac dysfunction: Role of Foxo3A-Parkin-mediated mitophagy. Biochimica et biophysica acta Molecular basis of disease. 2017;1863:1973–83.
29. Zheng Y, Shi B, Ma M, Wu X, Lin X. The novel relationship between Sirt3 and autophagy in myocardial ischemia-reperfusion. Journal of cellular physiology. 2019;234:5488–95.
30. Yu W, Dittenhafer-Reed KE, Denu JM. SIRT3 protein deacetylates isocitrate dehydrogenase 2 (IDH2) and regulates mitochondrial redox status. J Biol Chem. 2012;287:14078–86.
31. Agrotis A, Pengo N, Burden JJ, Ketteler R. Redundancy of human ATG4 protease isoforms in autophagy and LC3/GABARAP processing revealed in cells. Autophagy. 2019;15:976–97.
32. Aguirre L, Portillo MP, Hijona E, Bujanda L. Effects of resveratrol and other polyphenols in hepatic steatosis. World journal of gastroenterology. 2014;20:7366–80.
33. Masterjohn C, Bruno RS. Therapeutic potential of green tea in nonalcoholic fatty liver disease. Nutrition reviews. 2012;70:41–56.
34. Valenti L, Riso P, Mazzocchi A, Porrini M, Fargion S, Agostoni C. Dietary anthocyanins as nutritional therapy for nonalcoholic fatty liver disease. Oxidative Med Cell Longev. 2013;2013:145421.
35. Hale AN, Ledbetter DJ, Gawriluk TR, Rucker EB 3. Autophagy: regulation and role in development. Autophagy. 2013;9:951–72. rd. .
36. Kwanten WJ, Martinet W, Michielsen PP, Francque SM. Role of autophagy in the pathophysiology of nonalcoholic fatty liver disease: a controversial issue. World journal of gastroenterology. 2014;20:7325–38.
37. Gual P, Gilgenkrantz H, Lotersztajn S. Autophagy in chronic liver diseases: the two faces of Janus. American journal of physiology Cell physiology. 2017;312:C263-c73.
38. Kim TS, Jin YB, Kim YS, Kim S, Kim JK, Lee HM, et al. SIRT3 promotes antimycobacterial defenses by coordinating mitochondrial and autophagic functions. Autophagy. 2019;15:1356–75.
39. Lee J, Kim Y, Liu T, Hwang YJ, Hyeon SJ, Im H, et al. SIRT3 deregulation is linked to mitochondrial dysfunction in Alzheimer's disease. Aging cell. 2018;17.
40. Dikalova AE, Itani HA, Nazarewicz RR, McMaster WG, Flynn CR, Uzhachenko R, et al. Sirt3 Impairment and SOD2 Hyperacetylation in Vascular Oxidative Stress and Hypertension. Circulation research. 2017;121:564–74.
41. Zhou X, Chen M, Zeng X, Yang J, Deng H, Yi L, et al. Resveratrol regulates mitochondrial reactive oxygen species homeostasis through Sirt3 signaling pathway in human vascular endothelial cells. Cell death disease. 2014;5:e1576.
42. Kong-Hap MA, Mouammine A, Daher W, Berry L, Lebrun M, Dubremetz JF, et al. Regulation of ATG8 membrane association by ATG4 in the parasitic protist Toxoplasma gondii. Autophagy.

2013;9:1334–48.

43. Scherz-Shouval R, Shvets E, Fass E, Shorer H, Gil L, Elazar Z. Reactive oxygen species are essential for autophagy and specifically regulate the activity of Atg4. EMBO J. 2007;26:1749–60.
44. Betin VM, MacVicar TD, Parsons SF, Anstee DJ, Lane JD. A cryptic mitochondrial targeting motif in Atg4D links caspase cleavage with mitochondrial import and oxidative stress. Autophagy. 2012;8:664–76.
45. Kaminskyy VO, Zhivotovsky B. Free radicals in cross talk between autophagy and apoptosis. Antioxid Redox Signal. 2014;21:86–102.

Figures

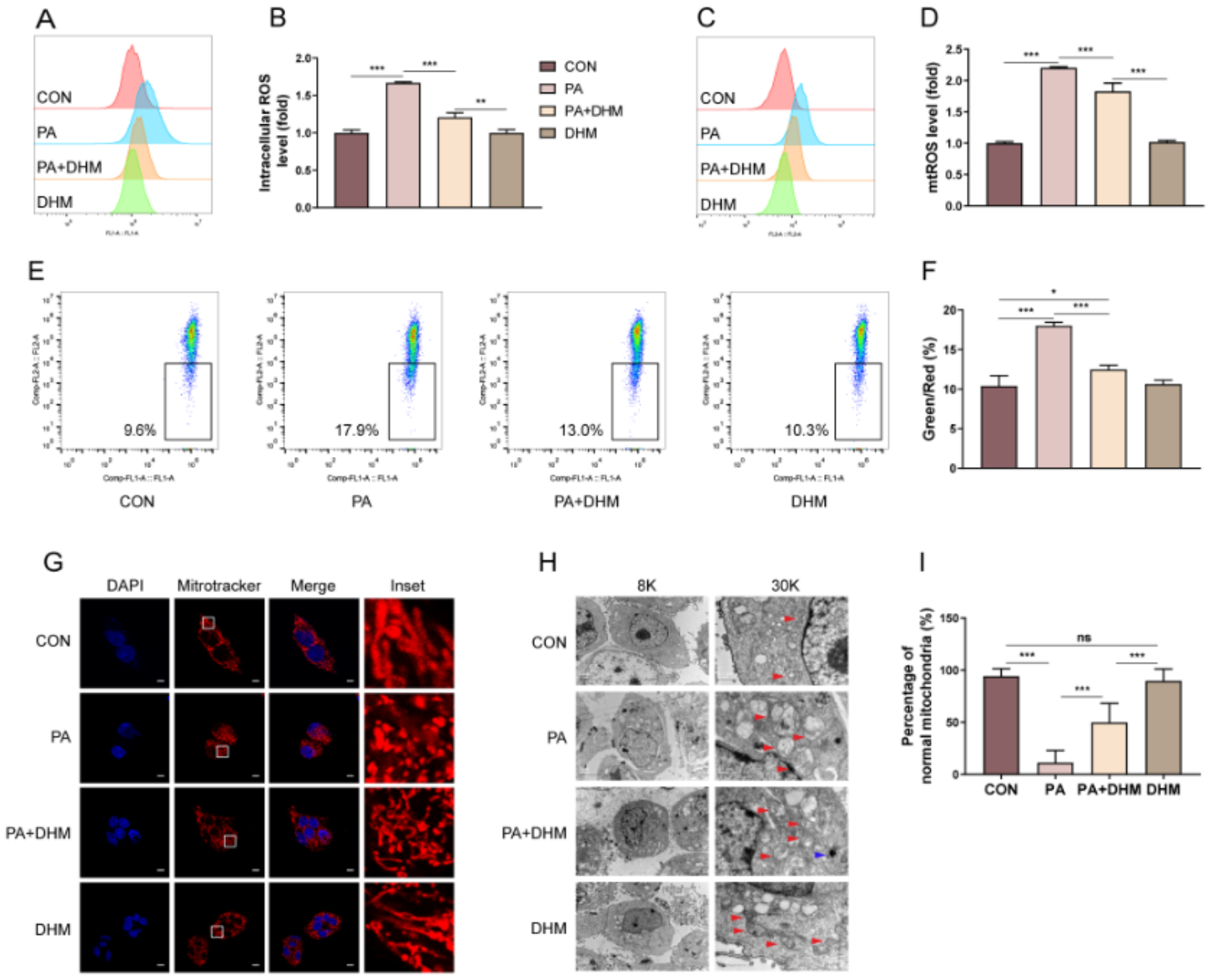

Figure 1

DHM inhibits PA-induced oxidative stress in hepatocytes. HepG2 cells were pretreated with 20 μM of DHM or the vehicle (0.5% DMSO) for 2 h, followed by the treatment of 0.2 mM of PA for an additional 16 h. (A-B) HepG2 cells were labeled with DCFH-DA probe and the intracellular ROS levels were measured by FCM assay. (C-D) HepG2 cells were labeled with MitoSOX™ Red probe and the mitochondria ROS (mtROS) levels were quantified by FCM assay. (E-F) HepG2 cells were labeled with JC-1 probe and the MMP level was quantified by FCM assay. (G) HepG2 cells were stained with MitoTracker Red and counterstained with DAPI. Representative images were acquired by a laser scanning confocal microscope, scale bars: 10 μm. (H) Representative TEM images of HepG2 cells at magnification of 8, 000× (left) and 30, 000× (right). The red arrows indicate mitochondria, and the blue arrow indicates an autophagosome. (I) The percentage of normal mitochondria in TEM images. Graphs showed mean ± SEM; n = 3; data were from one experiment out of three. * $p < 0.05$, ** $p < 0.01$, *** $p < 0.001$, compared between the marked groups; ns, no significant difference.

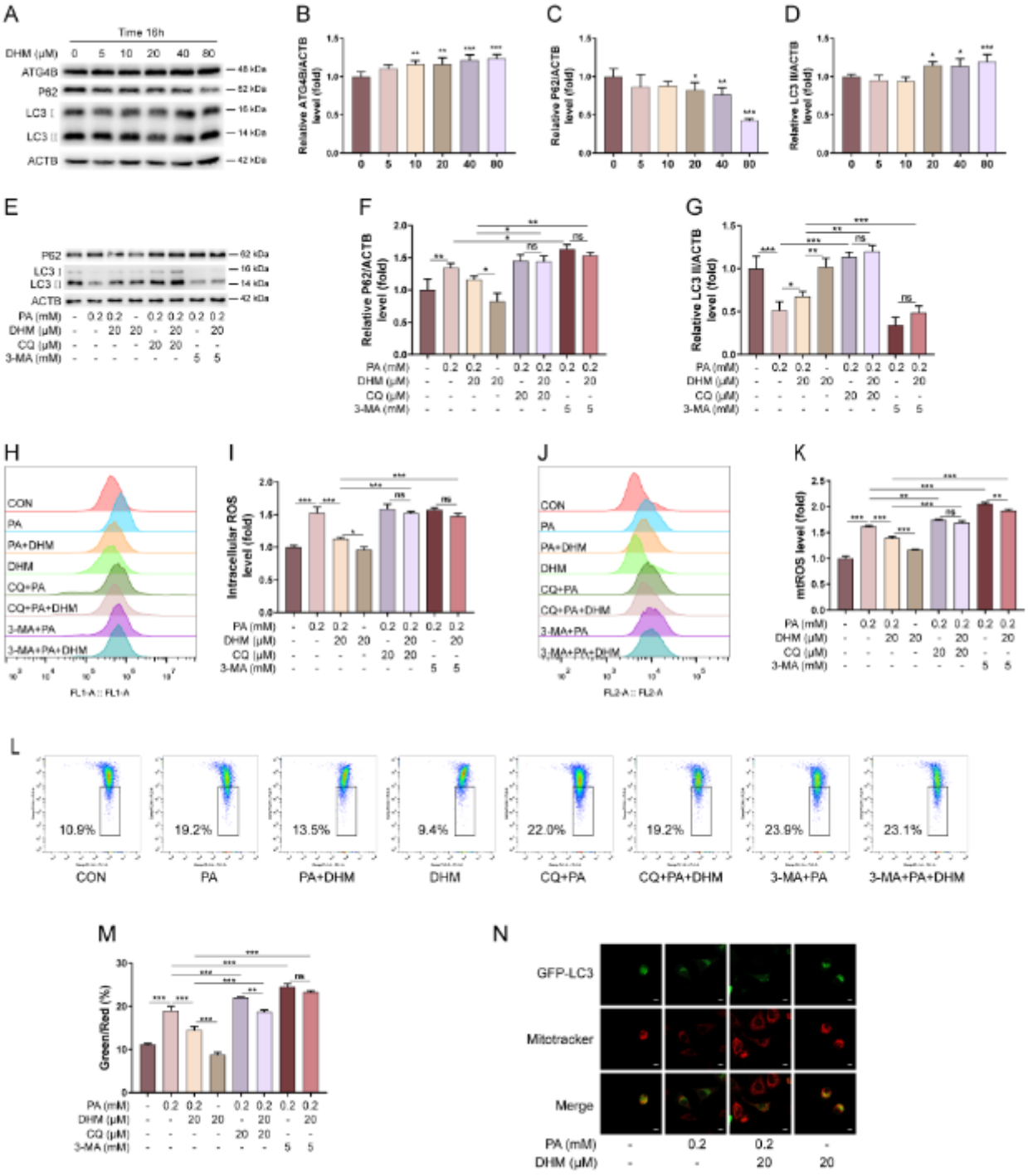

Figure 2

DHM suppresses PA-induced oxidative stress by induction of autophagy in hepatocytes. (A-D) HepG2 cells were treated with DHM of different concentrations (0, 5, 10, 20, 40 and 80 μM) for 16 h. The expressions of ATG4B, P62, and LC3 were analyzed by western blotting. Representative photographs (A) and densitometric quantification of ATG4B (B), P62 (C) and LC3 (D). (E-G) HepG2 cells were pretreated with CQ (20 μM) or 3-MA (5 mM) for 1 h, and then treated with DHM (20 μM) for 2 h followed by the exposure to PA (0.2 mM) for 16 h. The expressions of P62 and LC3 were analyzed by western blotting (E). The bar graphs showed the quantification of P62 (F) and LC3 (G), respectively. (H-I) HepG2 cells were

treated as indicated. The intracellular ROS level was analyzed by FCM assay (H), and the bar graph showed the quantification. (J-K) HepG2 cells were treated as indicated. The mtROS were analyzed by FCM assay (J) and the bar graph showed the quantification (K). (L-M) The MMP levels were analyzed by FCM assay (L) and the bar graph showed the quantification (M). (N) HepG2 cells were transfected with the GFP-LC3 expression vector for 4 h, followed by the treatment with DHM (20 μM) for 2 h and 0.2 mM of PA for an additional 16 h. Representative images of cells co-expressing MitoTracker Red and GFP-LC3 were showed by confocal microscopy; scale bars: 10 mm. Graphs showed mean ± SEM; n = 3; data were from one experiment out of three. * p < 0.05, ** p < 0.01, *** p < 0.001, compared between the marked groups; ns, no significant difference.

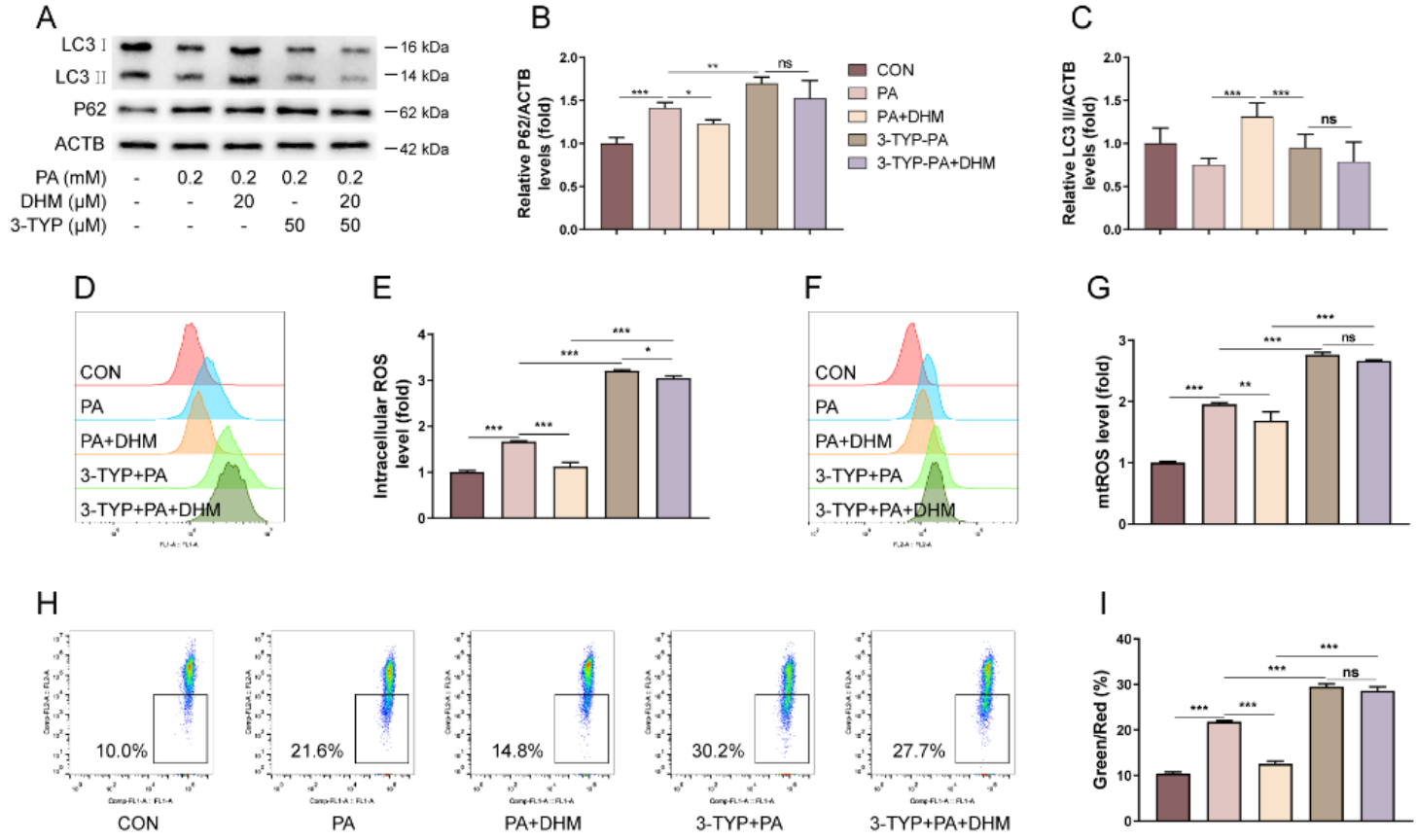

Figure 3

DHM attenuates PA-induced autophagy arrest and oxidative stress in hepatocytes via SIRT3. HepG2 cells were pretreated with 3-TYP (50 μM) or the vehicle for 1 h, followed by the treatment with DHM (20 μM) for 2 h and 0.2 mM of PA for 16 h. (A-C) Western blotting analysis of P62 and LC3 (A), and the densitometric quantification of P62 (B) and LC3 (C). (D-E) The intracellular ROS levels were measured by FCM assay (D), and the bar chart showed the quantification (E). (F-G) The mtROS levels were measured by FCM assay (F), and the bar chart showed the quantification (G). (H-I) The MMP levels were measured by FCM assay (H) and the bar chart showed the quantification (I). Graphs showed mean ± SEM; n = 3; data were from one experiment out of three. * p < 0.05, ** p < 0.01, *** p < 0.001, compared between the marked groups; ns, no significant difference.

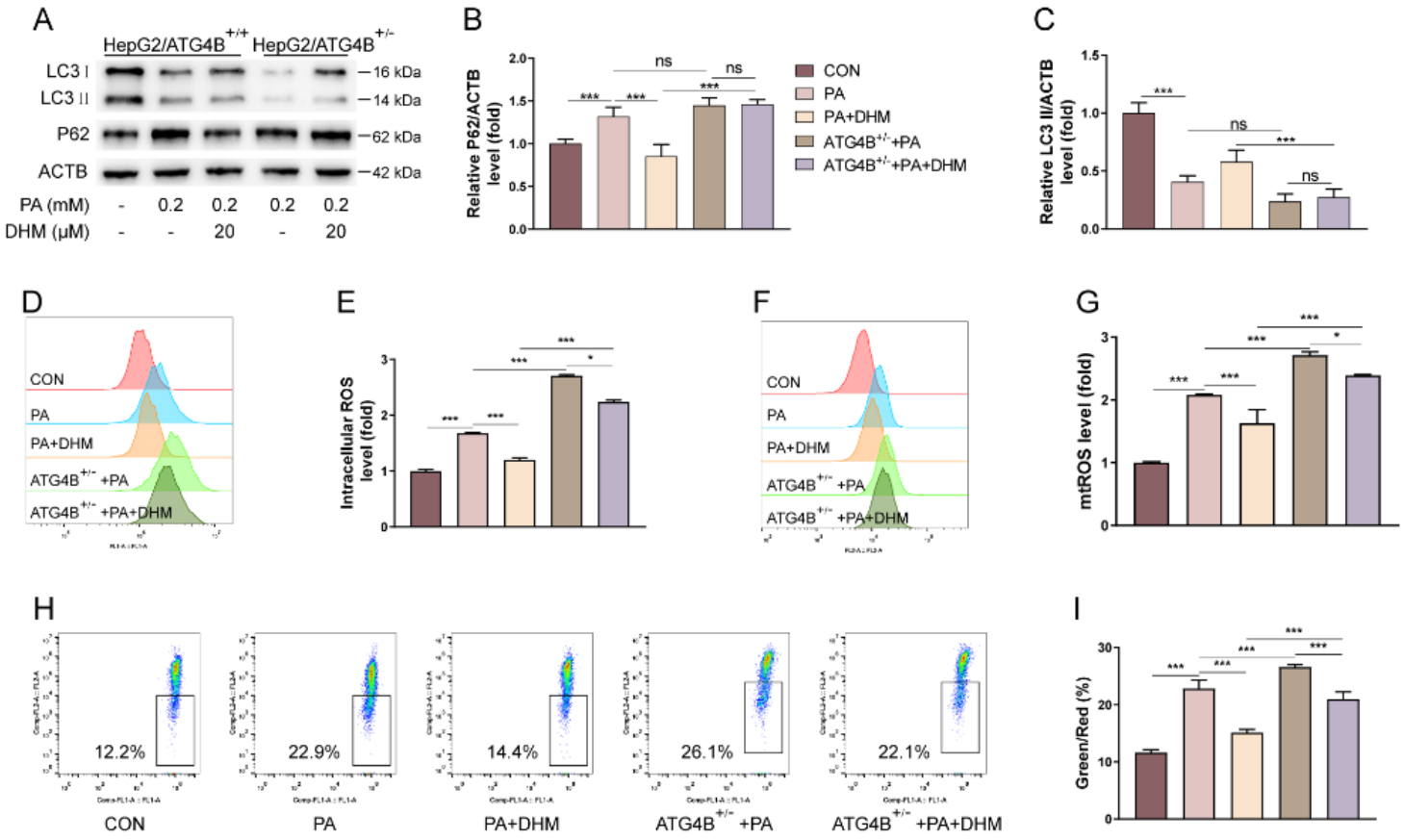

Figure 4

DHM attenuates PA-induced autophagy arrest and oxidative stress in hepatocytes partially through ATG4B. The HepG2 cells with ATG4B expression (HepG2/ATG4B+/+) and silencing ATG4B (HepG2/ATG4B+/−) were treated as indicated. (A-C) The expression of P62 and LC3 were analyzed by western blotting (A). And the bar graphs showed the quantification of P62 (B) and LC3 (C). (D-E) The intracellular ROS levels were measured by FCM assay (D) and quantified (E). (F-G) The mtROS levels were analyzed by FCM (F) and quantified (G). (H-I) The MMP levels were measured by FCM assay (H) and quantified (I). Graphs showed mean ± SEM; n = 3; data were from one experiment out of three. * $p < 0.05$, ** $p < 0.01$, *** $p < 0.001$, compared between the marked groups; ns, no significant difference.

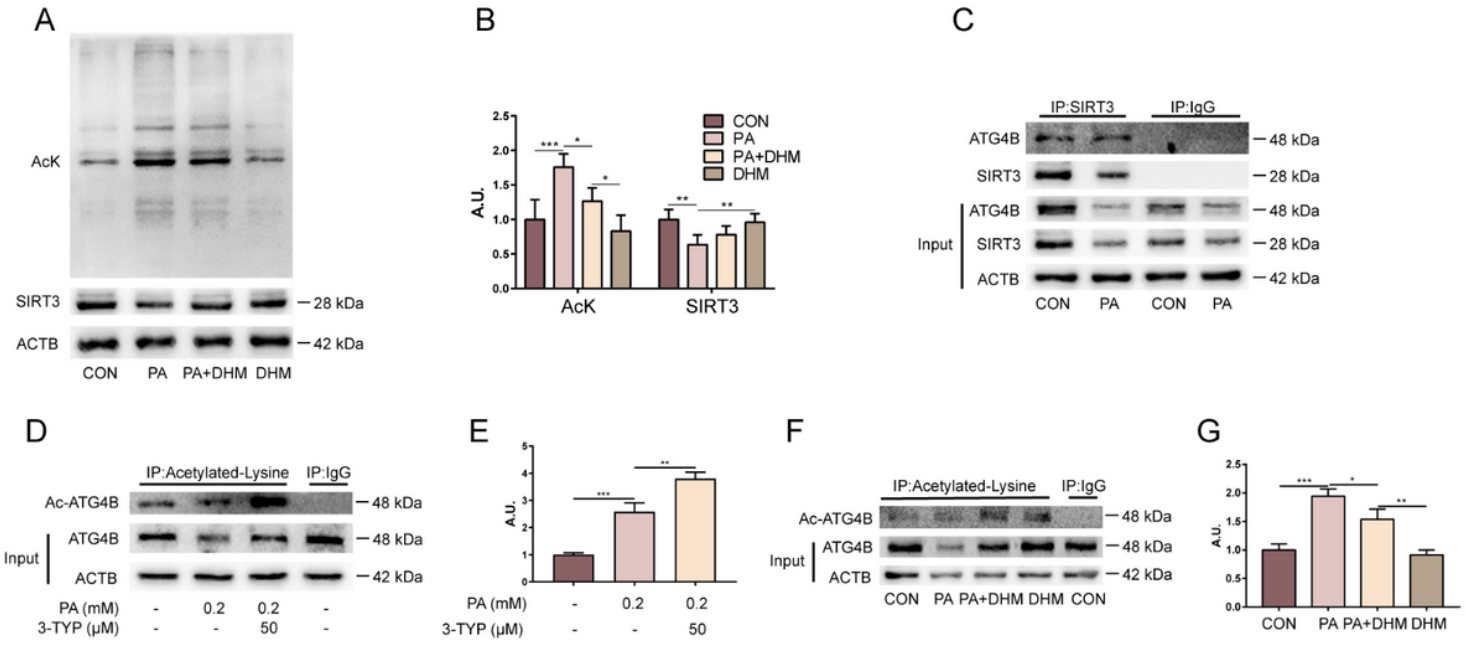

Figure 5

DHM facilitates SIRT3-mediated deacetylation of ATG4B in hepatocytes. (A-B) Western blotting analysis of total protein acetylation using anti-acetyllysine antibody (AcK) and the protein expression of SIRT3 (A). The bar chart showed the quantification (B). (C) The expression of ATG4B followed by co-immunoprecipitated with the anti-SIRT3 antibody was analyzed by western blotting. (D-E) HepG2 cells were pretreated with 3-TYP (50 μM) and then treated with PA (0.2 mM). The expressions of the acetylated and total ATG4B in HepG2 cells were measured by western blotting (D). The densitometric quantification of the ratio of acetylated-ATG4B/ATG4B (E). (F-G) HepG2 cells were treated with DHM and followed by PA treatment. The expressions of the acetylated and total ATG4B in HepG2 cells were analyzed by western blotting (F). The bar graph showed the quantification of the ratio of acetylated-ATG4B/ATG4B (G). Graphs showed mean ± SEM; n = 3; data were from one experiment out of three. *p < 0.05, **p < 0.01, ***p < 0.001, compared between the marked groups; A.U., arbitrary units.

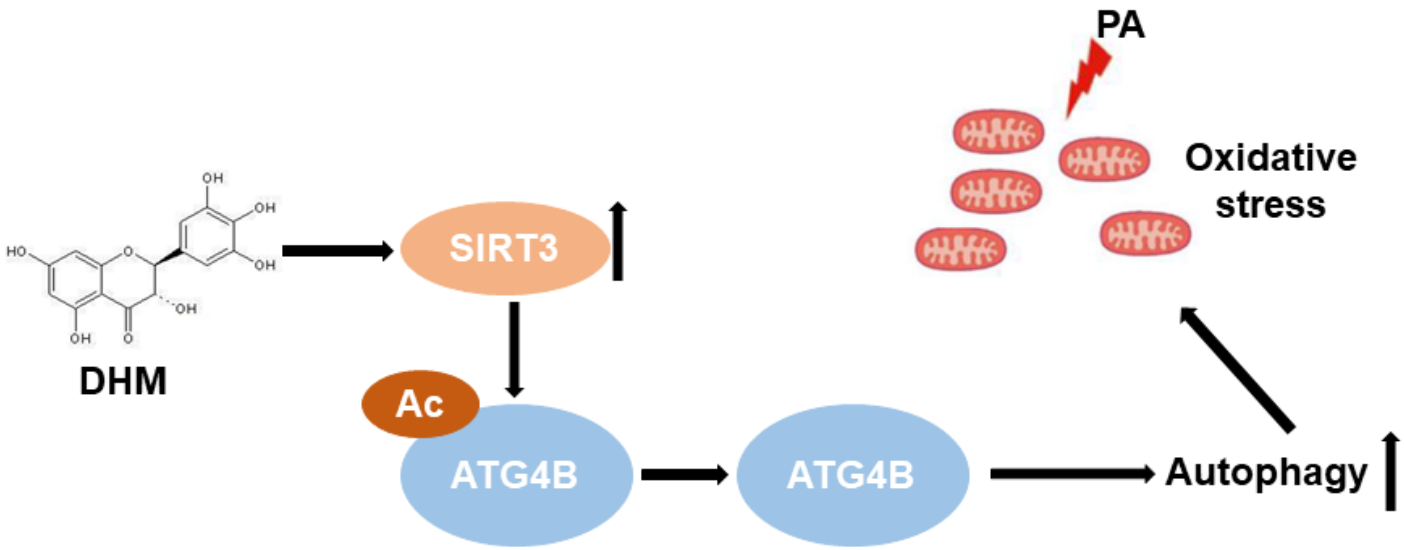

Figure 6

Schematic diagram of DHM-mediated amelioration of oxidative stress through induction of autophagy via a SIRT3–ATG4B signaling pathway in PA-treated hepatocytes. DHM attenuates PA-induced oxidative stress in hepatocytes through induction of autophagy, which is mediated through the increased expression of SIRT3 and SIRT3-mediated ATG4B deacetylation following DHM treatment.

Supplementary Files

This is a list of supplementary files associated with this preprint. Click to download.

- Supplementalfig1.tif
- Supplementalfig2.tif